AD

FATIGUE LIFE ASSESSMENT OF STEEL PRESSURE VESSELS WITH VARYING STRESS CONCENTRATION, RESIDUAL STRESS, AND INITIAL CRACKS

J. H. UNDERWOOD
A. P. PARKER

19961028 086

JULY 1996

US ARMY ARMAMENT RESEARCH,
DEVELOPMENT AND ENGINEERING CENTER
CLOSE COMBAT ARMAMENTS CENTER
BENÉT LABORATORIES
WATERVLIET, N.Y. 12189-4050

DTIC QUALITY INSPECTED 1

DISCLAIMER

The findings in this report are not to be construed as an official Department of the Army position unless so designated by other authorized documents.

The use of trade name(s) and/or manufacturer(s) does not constitute an official indorsement or approval.

DESTRUCTION NOTICE

For classified documents, follow the procedures in DoD 5200.22-M, Industrial Security Manual, Section II-19 or DoD 5200.1-R, Information Security Program Regulation, Chapter IX.

For unclassified, limited documents, destroy by any method that will prevent disclosure of contents or reconstruction of the document.

For unclassified, unlimited documents, destroy when the report is no longer needed. Do not return it to the originator.

REPORT DOCUMENTATION PAGE

Public reporting burden for this collection of information is estimated to average 1 hour per response, including the time for reviewing instructions, searching existing data sources, gathering and maintaining the data needed, and completing and reviewing the collection of information. Send comments regarding this burden estimate or any other aspect of this collection of information, including suggestions for reducing this burden, to Washington Headquarters Services, Directorate for Information Operations and Reports, 1215 Jefferson Davis Highway, Suite 1204, Arlington, VA 22202-4302, and to the Office of Management and Budget, Paperwork Reduction Project (0704-0188), Washington, DC 20503.

1. AGENCY USE ONLY (Leave blank)	2. REPORT DATE	3. REPORT TYPE AND DATES COVERED
	July 1996	Final

4. TITLE AND SUBTITLE
FATIGUE LIFE ASSESSMENT OF STEEL PRESSURE VESSELS WITH VARYING STRESS CONCENTRATION, RESIDUAL STRESS, AND INITIAL CRACKS

5. FUNDING NUMBERS
AMCMS No. 6111.02.H611.1

6. AUTHOR(S)

J.H. Underwood and A.P. Parker (Royal Military College of Science, Cranfield University, Swindon, UK)

7. PERFORMING ORGANIZATION NAME(S) AND ADDRESS(ES)
U.S. Army ARDEC
Benet Laboratories, AMSTA-AR-CCB-O
Watervliet, NY 12189-4050

8. PERFORMING ORGANIZATION REPORT NUMBER

ARCCB-TR-96022

9. SPONSORING/MONITORING AGENCY NAME(S) AND ADDRESS(ES)

U.S. Army ARDEC
Close Combat Armaments Center
Picatinny Arsenal, NJ 07806-5000

10. SPONSORING/MONITORING AGENCY REPORT NUMBER

11. SUPPLEMENTARY NOTES
To be presented at the 9th International Conference on Fracture, Sydney, Australia, 1-5 April 1997.
To be published in proceedings of the conference.

12a. DISTRIBUTION/AVAILABILITY STATEMENT

Approved for public release; distribution unlimited.

12b. DISTRIBUTION CODE

13. ABSTRACT (Maximum 200 words)

A single-parameter representation of local stress range, initial crack size, and material yield strength is proposed for describing the intensity of the fatigue loading of a structural component. A logarithmic plot of single-parameter fatigue life results provides a single straight-line description of fatigue life behavior over a broad range of material, configuration, and loading conditions. Expressions for calculating the local stress range at the failure site are outlined, including effects of vessel and stress concentrator configuration, applied and overstrain residual stresses, and pressure applied to hole and crack surfaces.

The single-parameter approach was used in a comparison of fatigue life results from 41 full-size hydraulic pressure cycle tests of cannon pressure vessels with 12 combinations of material strength, failure location, and applied and residual stresses. A log plot of mean results of the 12 data groups is well represented by a single straight line with a negative slope reasonably close to that predicted by fracture mechanics analysis. A significant outlier from the straight-line trend of the data is a useful indicator of cracking due to other than conventional mechanical fatigue. Two examples of an outlier from the trend of cannon pressure vessel data were confirmed by metallography to be caused by environmental cracking. A third outlier was related to preexisting initial cracks due to rapid machining.

The effect of material yield strength on fatigue behavior can be simply and well represented using the single-parameter approach. The R^2 correlation coefficient of a logarithmic straight-line fit to the 12 sets of cannon pressure vessel results increased from 0.81 to 0.86 upon inclusion of the effect of material strength.

14. SUBJECT TERMS	15. NUMBER OF PAGES
Metal Fatigue, Pressure Vessels, Fracture Mechanics, High-Strength Steels, Residual Stress, Fatigue Crack Growth, Stress Concentration, Stress-Life Curves	17
	16. PRICE CODE

17. SECURITY CLASSIFICATION OF REPORT	18. SECURITY CLASSIFICATION OF THIS PAGE	19. SECURITY CLASSIFICATION OF ABSTRACT	20. LIMITATION OF ABSTRACT
UNCLASSIFIED	UNCLASSIFIED	UNCLASSIFIED	UL

NSN 7540-01-280-5500

Standard Form 298 (Rev. 2-89)
Prescribed by ANSI Std. 239-18
298-102

TABLE OF CONTENTS

ACKNOWLEDGEMENTS

INTRODUCTION

The extensive testing of large high-strength steel cannon pressure vessels by Davidson et al. (ref 1) provides a baseline of fatigue lifetime information that would be difficult to match today. This work included significant variation in residual stresses and material strength and some known differences in initial crack size at the vessel inner radius, all of which have important effects on fatigue life. The experimental life results were assessed in terms of fracture mechanics, with emphasis on the range of stress intensity factor, ΔK, and fatigue life calculations as a function of ΔK. During the past two decades, additional life testing of cannon pressure vessels has been performed, with emphasis on fatigue failures that occur away from the vessel inner radius at various types of stress concentration and the associated analysis to understand and describe this type of fatigue failure.

Audino (ref 2) described a series of hydraulic pressure fatigue life tests in overstrained cannon tubes with failure locations both at the inner radius and at a notch in the outer radius. Underwood and Parker (ref 3) compared life results from overstrained cannon tubes containing erosion grooves at the inner radius with calculations using fracture mechanics. Underwood and coworkers (ref 4) analyzed several series of fatigue life tests of cannon tubes with various types of through-wall holes and different amounts of overstrain. Parker and coworkers (ref 5) performed fracture mechanics and fatigue life analyses for overstrained cannon tubes with axially-oriented holes and compared the analytical predictions with life tests.

Recent work by Parker and Underwood (ref 6) has proposed a simple new method for representing fatigue life results by accounting for two fundamentally important control variables for fatigue life - local stress range and initial crack size - in a single parameter. The objective of the work here is to use this single-parameter approach to describe the aforementioned fatigue lifetime results and thereby demonstrate its advantages and limitations in fatigue life analysis. The single-parameter approach will be briefly summarized and then used to describe the cannon pressure vessel results in a derivative of the conventional stress range versus life presentation. By including all the appropriate applied and residual stresses and the stress concentration in an expression for the local stress range, and by adding initial crack size and material strength information, the new single-parameter approach to fatigue life assessment is obtained. Critical comparisons of this single-parameter approach with the large body of cannon pressure vessel lifetime results should show whether or not the approach has broad utility in representing fatigue life of pressure vessels.

ANALYSIS

The general types of fatigue cracking of cannon pressure vessels considered here are shown schematically in Figure 1, along with some of the nomenclature. The single-parameter fatigue life analysis (ref 6) used to assess fatigue life for these various configurations is summarized, followed by the description of expressions for the local stress range at the site of fatigue cracking.
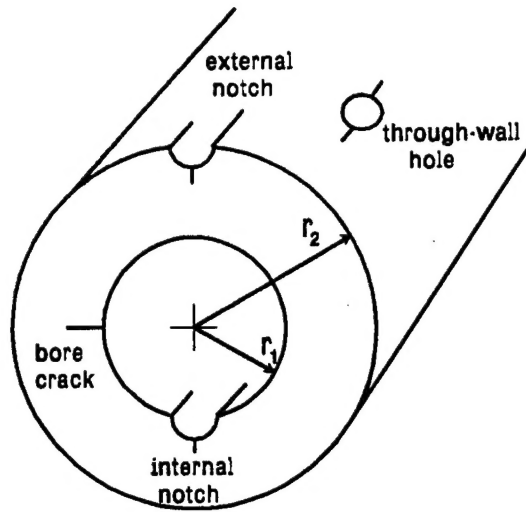
1

Fig. 1 - Some Types of Fatigue Cracking with Pressure Vessels

Single-Parameter Fatigue Life Analysis

The Paris law (ref 7) describes a significant portion of the fatigue crack growth behavior, da/dN, of most metals

$$da/dN = C(\Delta K)^m \tag{1}$$

where ΔK is the positive range of stress intensity factor and C and m are experimental constants. For steels m is often about 3. A general expression for ΔK is

$$\Delta K = \Delta \sigma (\pi a)^{1/2} \tag{2}$$

where $\Delta \sigma$ includes the constant, often near 1, relating to crack configuration. Combining Eqs. (1) and (2) and integrating over the range from the initial crack size, a_i, to the critical crack size, a_c, gives

$$N = [1/(C\pi^{m/2}\{1-m/2\}\{\Delta\sigma\}^m)][a_c^{(1-m/2)} - a_i^{(1-m/2)}] \tag{3}$$

which is the basis of the work by Maddox (ref 8) relating the Paris law to the conventional log $\Delta \sigma$ versus log N fatigue life presentation. Recognizing that the second term is constant for a given a_i and that typically $a_c \gg a_i$, taking logs leads to

$$\log(\Delta\sigma) = (-1/m)\log N + (1/m - 1/2)\log a_i - (1/m)\log\{(m/2-1)C\pi^{m/2}\} \tag{4}$$

Finally, rearranging Eq. (4) leads to

$$\log(\Delta\sigma \times a_i^{(1/2-1/m)}) = (-1/m)\log N - (1/m)\log\{(m/2-1)C\pi^{m/2}\} \tag{5}$$

2

which can be recognized as a straight line on log coordinates with slope $(-1/m)$ and intercept $-(1/m)\log\{(m/2 -1)C\pi^{m/2}\}$, which are constant for a given material. The form of Eq. (5) suggests that plots of $\log \Delta\sigma$ versus $\log N$ will fall on a single straight line with $(-1/m)$ slope and that all the critical stress range and initial crack size information will be included in the single parameter $(\Delta\sigma \times a_i^{(\frac{1}{2} - 1/m)})$. If this proves to be true over a significant range of fatigue lifetime test conditions, it will be a useful method for fatigue life assessment.

Local Stress Range for Control of Fatigue Cracking

An expression for the local stress range, $\Delta\sigma$, that includes the important stresses for all the types of fatigue cracking considered here is as follows:

$$\Delta\sigma = k_{t\text{-}\theta}\sigma_\theta + k_{t\text{-}ov}\sigma_{ov} - \sigma_r + p_{hole} + p_{crack} \tag{6}$$

The first two terms represent the stresses that often have the primary control of fatigue cracking in a pressure vessel, the applied and residual (due to overstrain) hoop direction stresses at the crack initiation site, σ_θ and σ_{ov}, sometimes multiplied by stress concentration factors, $k_{t\text{-}\theta}$ and $k_{t\text{-}ov}$, if a stress raiser is present. The third term accounts for the indirect effect of the compressive radial direction stress, σ_r, that, in a few cases here with a notch present, effectively adds to the tensile hoop stress at certain locations around the notch. For example, at the crack locations in the internal and external notch radii shown in Figure 1, the tensile hoop stress is increased by the (negative) value of the compressive radial stress at these locations. Near the vessel inner radius this effect of radial stress effectively adding to the hoop stress is significant. The last two terms in Eq. (6) account for the additional effect of pressure in the hole or in the crack. Pressure in a hole produces a tensile hoop stress at the hole inner radius with magnitude of about the value of pressure applied to the vessel. Pressure in the crack produces the equivalent of a tensile stress oriented normal to the crack plane that is also equal in magnitude to the applied pressure. So these two additional pressure effects, which add to the stresses in the vessel wall, can have significant control over fatigue life.

The expression used to calculate stress concentration factor at a notch is as follows, from Roark and Young (ref 9):

$$k_t = 1 + 2c/b \tag{7}$$

where c is the depth of a semielliptically shaped notch and b is the half-width of the notch.

The local positive stress range is calculated from Eqs. (6) and (7) at the site of fatigue cracking and is used in the single-parameter presentation of fatigue life results as discussed in relation to Eq. (5), that is, a plot of $\Delta\sigma \times a_i^{(\frac{1}{2} - 1/m)}$ versus N. These results are presented in the following section, with emphasis on the effects of overstrain residual stress, initial crack size, stress concentration, and material yield strength on the single-parameter representation of fatigue lifetime.

RESULTS

Fatigue Failure at the Vessel Bore

A conventional $\Delta\sigma$ versus N plot of results from 24 cannon pressure vessel fatigue life tests is shown in Figure 2 for fired (500 cannon firings typical before hydraulic pressure cycles) and unfired cannon tubes with and without overstrain residual stress. Table 1 lists key information from the tests, including the mean life for each of six types of vessels. The failure location for these 24 tests was at the 0.5-mm root radius of one of the 1.8-mm high rifling lands at the bore of the cannon tube. The stress concentration factor at the rifling radius was included in the Eq. (6) calculations of $\Delta\sigma$ by setting $k_{t-\theta} = 1.7$, so that the applied stresses were increased by this factor. No increase in the residual stresses was made, that is, $k_{t-ov} = 1.0$, based on the belief that any potential increase in the residual stress at the rifling radius would have been relieved by the machining of the rifling or by yielding at the root radius of the rifling. Expressions for the applied and residual stresses in the vessel, σ_θ and σ_{ov}, were obtained from Roark and Young (ref 9) and Hill (ref 10), respectively. The σ_r and p_{hole} terms do not apply to bore cracks so they were not used.

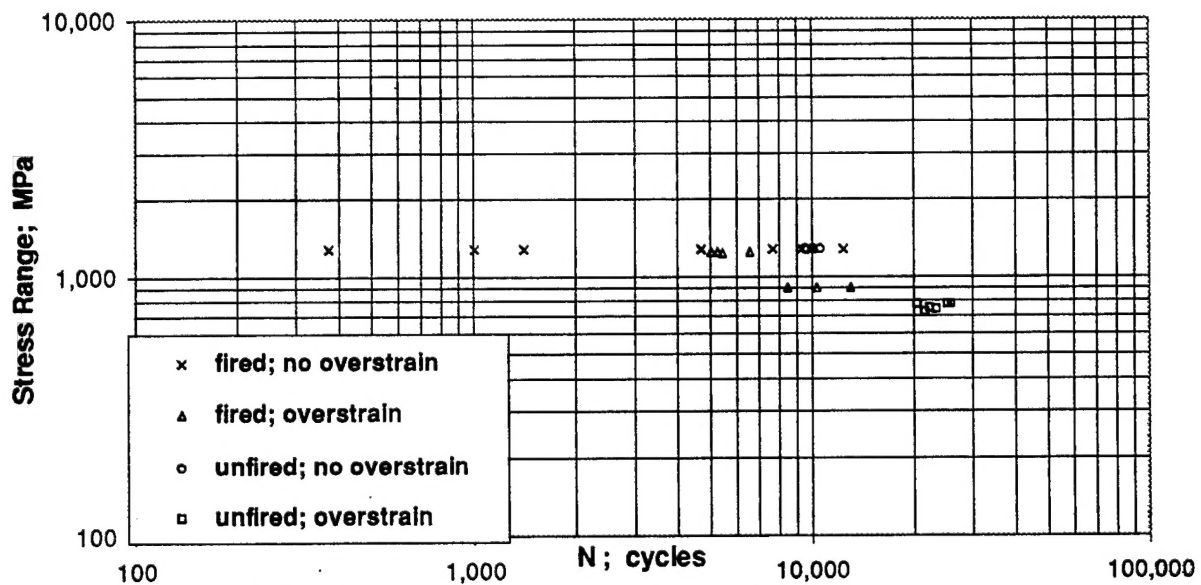Fig. 2 - Effect of Bore Stress Range on Cannon Fatigue Life

4

Table 1. Vessels with Fatigue Failure at the Bore; see Figures 2 and 3

Type/Number of Vessels	Yield Strength MPa	Inner Radius mm	Outer Radius mm	Applied Pressure MPa	Stress Range MPa	Fatigue Life cycles	Initial Crack mm
FIRED; NO OVERSTRAIN							
a 3	1200	89	187	345	1275	10,039	0.1
b 4	1270	89	187	345	1275	4,110	0.5
1	1180	89	187	345	1275	373	> 0.5
FIRED; OVERSTRAIN							
c 4	1120	79	155	. 670	1247	5,590	0.1
d 3	1230	89	142	393	896	10,629	0.1
UNFIRED; NO OVERSTRAIN							
e 3	1280	89	187	345	1275	10,094	0.01
UNFIRED; OVERSTRAIN							
f 6	1020	89	187	345	758	23,152	0.01

The results in Figure 2 are logical in some respects. The fired cannon tubes have generally lower lives than the unfired, and the overstrained cannon tubes have generally higher lives than those with no overstrain. However, the overall trend is a significant variation in fatigue life, while stress range is relatively constant. This suggests that another important variable that controls fatigue life should be considered, such as the initial crack size. Table 1 lists the variations in initial crack size that are known to have been present in these tubes. Unfired tubes have naturally-occurring inclusions or surface roughness corresponding to about 0.01-mm deep initial cracks, whereas fired tubes typically have 0.1-mm deep heat check cracks. The group *b* fired tubes were found to have unusually deep heat check cracks of about 0.5-mm, and metallographic tests showed that one group *b* tube had an even deeper initial crack, discussed later.

The bore failure results are replotted in Figure 3 by using the single parameter discussed earlier to account for the differences in initial crack size. The stress range has been modified to include $a_i^{(\frac{1}{2} - 1/m)}$ which, for m = 3, becomes $a_i^{1/6}$. Values of a_i in meters were used to calculate $(\Delta\sigma \times a_i^{1/6})$. Note that the single-parameter plotting of the results shows a somewhat more consistent trend toward an increase in life with a decrease in $\Delta\sigma \times a_i^{1/6}$. Also, it is easier to see in this plot that the fired tube results include considerably more variation than the unfired tube results. This is caused by the variation in the number and type of cannon firings performed before the hydraulic pressure cycles. The overall trend of the results follows the arbitrary line with slope = -1/3, but with the variation noted above.
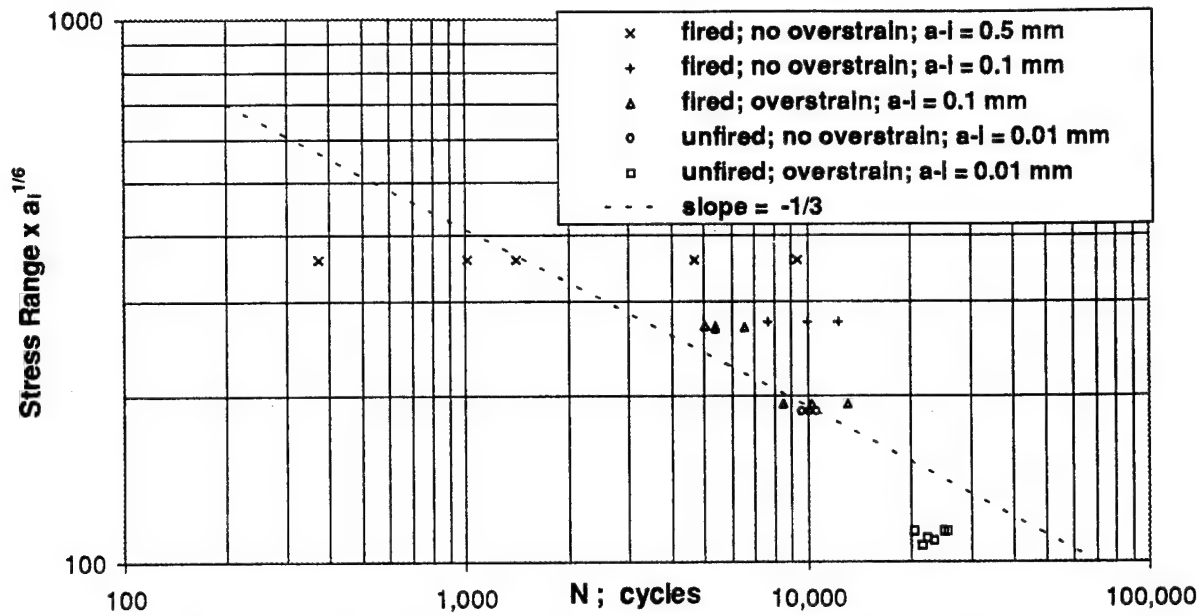
Fig. 3 - Effect of Bore Stress Range and Initial Crack Size on Life

Fatigue Failure at a Stress Concentrator

Results from another group of 17 cannon pressure vessels, each with fatigue failure at a significant stress concentrator, are shown in Figure 4 and Table 2. Various notch and through-wall hole configurations of the types shown in Figure 1 were tested. The through-wall holes were 2-mm in diameter oriented at 30 degrees to the vessel axis to allow exit of the cannon combustion gasses. The Eq. (6) calculations for the vessels with holes included the $k_{t \cdot \theta} \sigma_\theta$, p_{hole}, and p_{crack} terms; the other two terms do not affect $\Delta\sigma$. The calculations for external and mid-wall notches included the $k_{t \cdot \theta} \sigma_\theta$ and σ_r terms; the calculations with internal notches included all terms in Eq. (6). The values of k_t for the hole and the semicircular midwall notches were based on the known value of 3, with a reduction in the case of the midwall notches because of their close spacing. The values of k_t for the external and internal notches were from Eq. (7).
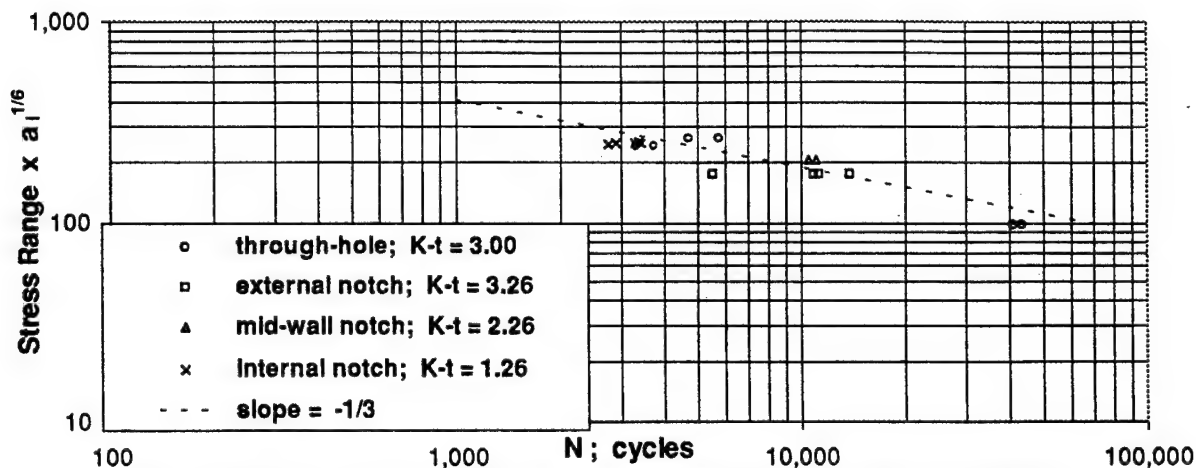
Fig. 4 - Effect of Nominal Stress Range, Stress Concentration and Initial Crack Size on Fatigue Life

Legend in figure:
- o through-hole; K-t = 3.00
- □ external notch; K-t = 3.26
- ▲ mid-wall notch; K-t = 2.26
- × Internal notch; K-t = 1.26
- - - - slope = -1/3

Y-axis: Stress Range × $a_i^{1/6}$
X-axis: N ; cycles

Table 2. Vessels with Fatigue Failure at a Stress Concentrator; see Figure 4

Type/Number of Vessels		Yield Strength MPa	Inner Radius mm	Outer Radius mm	Applied Pressure MPa	Stress Range MPa	Fatigue Life cycles	Initial Crack mm
THROUGH-HOLE; $K_t = 3.00$								
g	2	1240	53	76	207	1797	5,240	0.01
h	2	1170	60	94	297	1657	5,535	0.01
I	2	1220	78	107	83	664	42,025	0.01
EXTERNAL NOTCH; $K_t = 3.26$								
j	3	1230	78	142	393	1196	11,960	0.01
	1	1240	78	142	393	1196	5,501	>0.01
MID-WALL NOTCH; $K_t = 2.26$								
k	2	1240	85	153	406	1397	10,605	0.01
INTERNAL NOTCH; $K_t = 1.26$								
l	5	1070	60	135	670	1702	3,159	0.01

7

The results in Figure 4 for failure at a stress concentrator show a similar trend to the Figure 3 results for failure at the bore. As in Figure 3, there is a consistent trend toward an increase in life with a decrease in $\Delta\sigma \times a_i^{1/6}$, and the results are in approximate agreement with the same line with slope = -1/3 shown earlier.

Significant Variation in Initial Crack Size

Two of the cannon pressure vessel fatigue life results discussed thus far have included a known significant variation in initial crack size, one of the type b vessels in Table 1 and one of the type j vessels in Table 2. In addition to these, another significant variation from conventional mechanical fatigue cracking has recently been described by Troiano et al. (ref 11). These variations from the norm are considered in Figure 5 and Table 3. Figure 5 shows a ($\Delta\sigma \times a_i^{1/6}$) versus N plot of the comparison. The table shows the different types of failure and levels of stress range of the three examples, and it compares a_i and N for both the typical fatigue failures and the atypical failures.
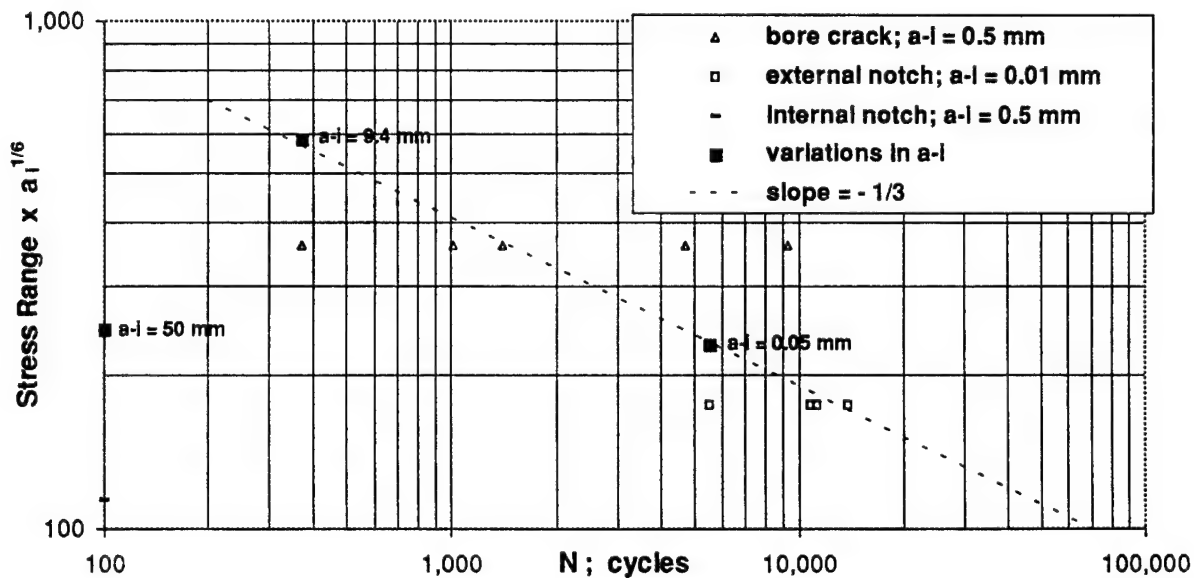

Fig. 5 - Effect of Significant Variations in Initial Crack Size on Life

8

Table 3. Vessels with Significant Variations in Initial Crack Size; see Figure 5

Type of Failure	Stress Range MPa	Fatigue Failure a_i mm	Fatigue Failure N cycles	Atypical Failure a_i mm	Atypical Failure N cycles	cause
Bore Crack	892	0.5	4,110	9.4	373	Environment
External Notch	1196	0.01	11,960	0.05	5,501	Machining
Internal Notch	405	0.5	48,000 CALCULATED	50	100	Environment

The bore crack test with variation in a_i included fractography results that showed evidence of environmental fracture. If the 9.4-mm crack present at failure had been wholly due to environmental cracking, the result shown in the plot would be in reasonable agreement with the -1/3 slope trend of the data.

The external notch test with variation in a_i also included a metallographic study that showed a 0.05-mm deep initial crack due to a rapid machining process, compared with the expected value of 0.01-mm in unaffected material. Note in Figure 5 that the use of the deeper crack based on metallographic results is in good agreement with the -1/3 slope trend of the data.

The last example of the effect of a significant variation in a_i on fatigue life provides the most striking results. Data from a 100-cycle life test reported by Troiano et al. (ref 11) is plotted in Figure 5, with $(\Delta\sigma \times a_i^{1/6})$ determined using $a_i = 0.5$-mm, the largest value that could be expected for normal cannon conditions. However, this plotted point is nearly three orders of magnitude away from the trend of the data. Even when the a_i value at the end of the test was used, $a_i = 50$-mm, the agreement is still poor. This is a clear indication that the cracking process that occurred with this vessel is nothing close to conventional mechanical fatigue, which adds to the indications of atypical failure reported by Troiano et al.

9

Variation in Material Yield Strength

It may be useful to consider a summary plot of all the results discussed thus far, keeping in mind that material yield strength, an important control variable for fatigue, has not yet been addressed. Figure 6 shows such a plot, which can be the basis for addressing yield strength effects. Twelve mean values of $(\Delta\sigma \times a_i^{1/6})$ and N are plotted, calculated from each of the twelve types of vessel data listed in Tables 1 and 2, designated a through l. The data with a_i variations discussed above were not included in the mean values. Considering the inherent variations in fatigue life tests, the trend of the summary of results of Figure 6 is quite consistent. Standard linear regression of $\log(\Delta\sigma \times a_i^{1/6})$ versus $\log N$ produced the line shown, with correlation coefficient $R^2 = 0.81$ and slope = -0.46.
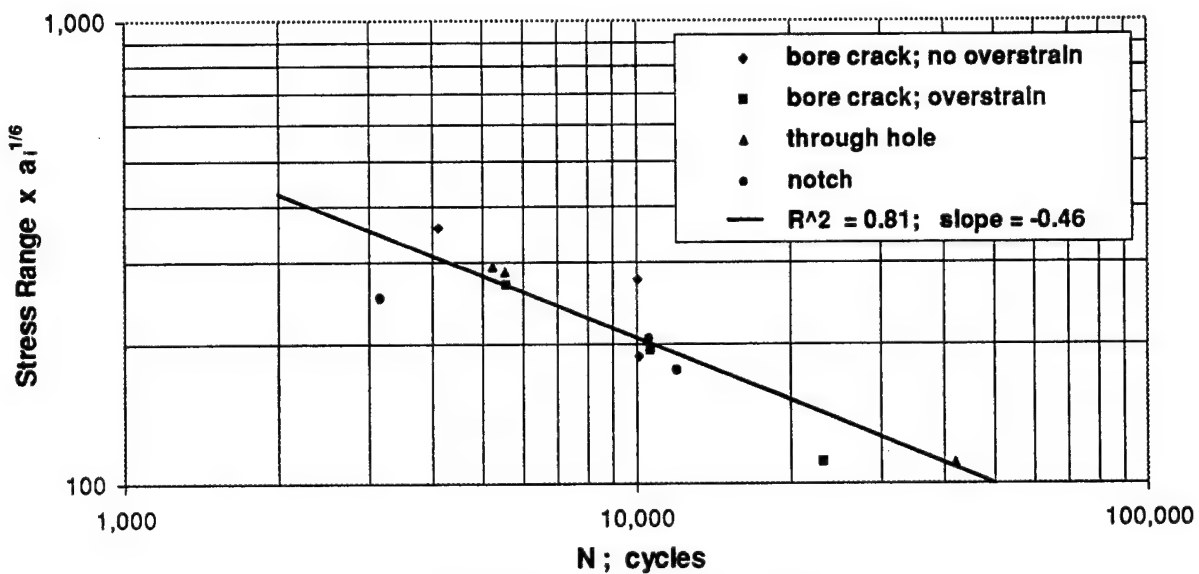

Fig. 6 - Comparison of Mean Life Results

The summary results of Figure 6 are presented in Figure 7 with a modification in the single parameter to account for the effect of material yield strength. The single-parameter representation of local stress range, initial crack size, and material yield strength takes the form

$$\text{fatigue intensity factor} = \Delta\sigma \times (S_{y\text{-ave}}/S_y) \times a_i^{1/6} \qquad (8)$$

Equation (8) is proposed as a parameter that describes the intensity of the fatigue loading of a structural component, including the important effect of material strength as well as the effects of stresses and initial crack at the failure site. The $(S_{y\text{-ave}}/S_y)$ term effectively increases the stress range for a specimen with yield strength lower than the mean value, and this is consistent with the shorter life expected for a decrease in strength. The $(S_{y\text{-ave}}/S_y)$ form has the advantage of approaching unity when there is little difference in strength.

Fig. 7 - Mean Life Results Including Yield Strength Effect
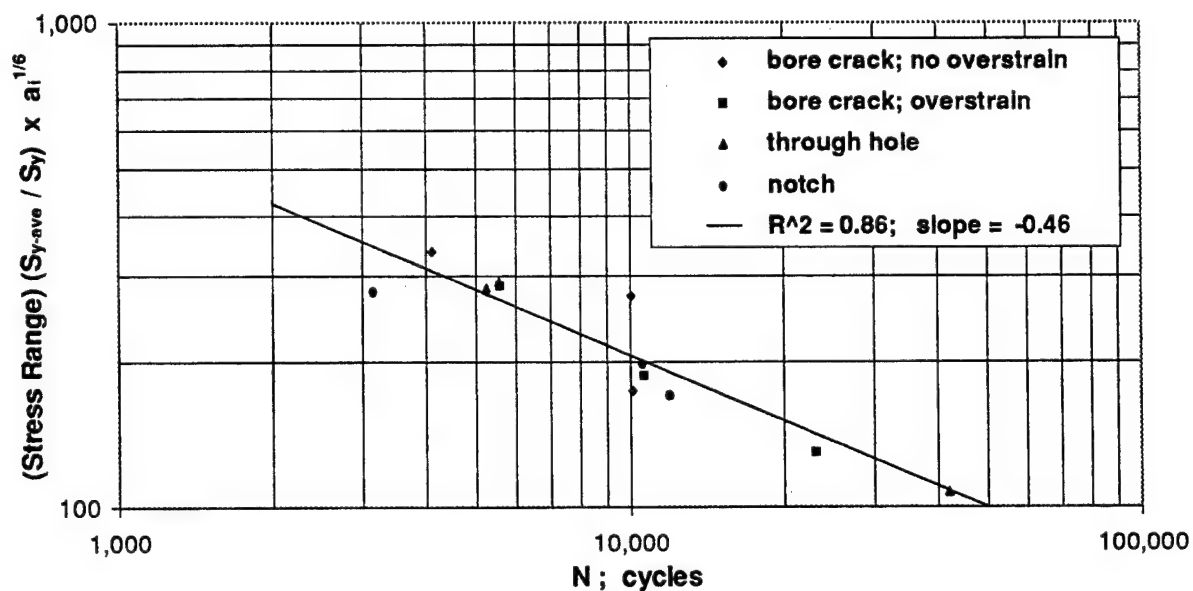
Note in Figure 7 that results for materials with strength most different from the mean strength moved closer to the regression line. This resulted in an increase in R^2 from 0.81 to 0.86, but no significant change in the position or slope of the regression line. This supports the inclusion of the material yield strength effect in the concept of fatigue intensity factor as proposed in Eq. (8).

Finally, it can be shown that a general form of the material strength effect in the single-parameter description of fatigue life is

$$\text{fatigue intensity factor} = \Delta\sigma \times (S_{y\text{-ave}}/S_y)^{2/m} \times a_i^{1/6} \tag{9}$$

The $(S_{y\text{-ave}}/S_y)^{2/m}$ term can be obtained by assuming that crack growth rate varies directly with the size of the crack-tip plastic zone, so that fatigue life varies inversely with zone size, that is, $N \propto (S_y/K)^2$. This $N \propto S_y^2$ relationship, when included in the log σ versus log N form with slope -1/m, leads to the $(S_{y\text{-ave}}/S_y)^{2/m}$ term in Eq. (9). It is interesting to note that for the value of m in Figure 7, about 2.2, Eq. (9) gives a value for the exponent of the $(S_{y\text{-ave}}/S_y)$ term of 1.1. This is close to the value of unity used in Eq. (8) to account for material strength.

SUMMARY AND CONCLUSIONS

A single-parameter representation of local stress range, initial crack size, and material yield strength is proposed for describing the intensity of the fatigue loading of a structural component. Use of this single parameter with logarithmic plots of fatigue lifetime provides a single straight-line description of fatigue life behavior over a broad range of material, configuration, and loading conditions.

Expressions for calculating the local stress range at the failure site are outlined, including effects of pressure vessel and stress concentrator configuration, applied and overstrain residual stresses, and pressure applied to hole and crack surfaces.

The single-parameter approach was used in a comprehensive comparison of fatigue life results from 41 full-size hydraulic pressure cycling tests of cannon pressure vessels with 12 combinations of material strength, failure location, and applied and residual stresses. A log plot of mean results of the 12 data groups is well represented by a single straight line with a negative slope reasonably close to that predicted by fracture mechanics analysis.

12

A significant outlier from a single-parameter plot of fatigue lifetime data is a useful indicator of cracking due to other than conventional mechanical fatigue. Two examples of an outlier from the trend of cannon pressure vessel data were confirmed by fractography to be caused by environmental cracking. A third outlier was related to preexisting initial cracks due to rapid machining.

The effect of material yield strength on fatigue behavior can be simply and well represented using the single-parameter approach. The R^2 correlation coefficient of a logarithmic straight-line fit to the 12 sets of cannon pressure vessel results increased from 0.81 to 0.86 upon inclusion of the effect of material strength.

13

REFERENCES

1. T.E. Davidson, J.F. Throop, and J.H. Underwood, in: *Case Studies in Fracture Mechanics*, (T.P. Rich and D.J. Cartwright, Eds.), Army Materials and Mechanics Research Center, Watertown, MA, 1977, pp. 3.9.1-3.9.13.

2. M.J. Audino, "Fatigue Life Assessment of 155-mm M284 Cannon Tubes," ARDEC Technical Report ARCCB-TR-93036, Benet Laboratories, Watervliet, NY, October 1993.

3. J.H. Underwood and A.P. Parker, *J. of Pressure Vessel Technology*, Vol. 117, 1995, pp. 222-226.

4. J.H. Underwood, A.P. Parker, D.J. Corrigan, and M.J. Audino, in: *PVP - Vol. 316, Plant Systems/Components Aging Management*, ASME, New York, 1995, pp. 154-161.

5. A.P. Parker, S.N. Endersby, T.J. Bond, J.H. Underwood, S.L. Lee, and J. Higgins, in: *Proceedings of PVP Conference (July 1996)*, ASME, New York, to be published.

6. A.P. Parker and J.H. Underwood, in: *Fatigue and Fracture Mechanics: Twenty-Eighth Volume, STP 1321*, American Society for Testing and Materials, Philadelphia, to be published.

7. P.C. Paris and F. Erdogan, *J. of Basic Engineering*, Vol. 85, 1963, pp. 528-534.

8. S.J. Maddox, "Fracture Mechanics Applied to Fatigue in Welded Structures," *Welding Institute Conference on Fatigue of Welded Structures*, Brighton, England, 1970, pp. 73-96.

9. R.J. Roark and W.C. Young, *Formulas for Stress and Strain*, McGraw-Hill, New York, 1975.

10. R. Hill, *The Mathematical Theory of Plasticity*, Clarendon Press, Oxford, 1950.

11. E. Troiano, J.H. Underwood, A. Scalise, G.P. O'Hara, and D. Crayon, in: *Fatigue and Fracture Mechanics: Twenty-Eighth Volume, STP 1321*, American Society for Testing and Materials, Philadelphia, to be published.

TECHNICAL REPORT INTERNAL DISTRIBUTION LIST

	NO. OF COPIES
CHIEF, DEVELOPMENT ENGINEERING DIVISION	
ATTN: AMSTA-AR-CCB-DA	1
-DB	1
-DC	1
-DD	1
-DE	1
CHIEF, ENGINEERING DIVISION	
ATTN: AMSTA-AR-CCB-E	1
-EA	1
-EB	1
-EC	1
CHIEF, TECHNOLOGY DIVISION	
ATTN: AMSTA-AR-CCB-T	2
-TA	1
-TB	1
-TC	1
TECHNICAL LIBRARY	
ATTN: AMSTA-AR-CCB-O	5
TECHNICAL PUBLICATIONS & EDITING SECTION	
ATTN: AMSTA-AR-CCB-O	3
OPERATIONS DIRECTORATE	
ATTN: SIOWV-ODP-P	1
DIRECTOR, PROCUREMENT & CONTRACTING DIRECTORATE	
ATTN: SIOWV-PP	1
DIRECTOR, PRODUCT ASSURANCE & TEST DIRECTORATE	
ATTN: SIOWV-QA	1

NOTE: PLEASE NOTIFY DIRECTOR, BENÉT LABORATORIES, ATTN: AMSTA-AR-CCB-O OF ADDRESS CHANGES.

TECHNICAL REPORT EXTERNAL DISTRIBUTION LIST

	NO. OF COPIES		NO. OF COPIES
ASST SEC OF THE ARMY RESEARCH AND DEVELOPMENT ATTN: DEPT FOR SCI AND TECH THE PENTAGON WASHINGTON, D.C. 20310-0103	1	COMMANDER ROCK ISLAND ARSENAL ATTN: SMCRI-SEM ROCK ISLAND, IL 61299-5001	1
DEFENSE TECHNICAL INFO CENTER ATTN: DTIC-OCP (ACQUISITIONS) 8725 JOHN J. KINGMAN ROAD STE 0944 FT. BELVOIR, VA 22060-6218	2	MIAC/CINDAS PURDUE UNIVERSITY 2595 YEAGER ROAD WEST LAFAYETTE, IN 47906-1398	1
COMMANDER U.S. ARMY ARDEC ATTN: AMSTA-AR-AEE, BLDG. 3022 AMSTA-AR-AES, BLDG. 321 AMSTA-AR-AET-O, BLDG. 183 AMSTA-AR-FSA, BLDG. 354 AMSTA-AR-FSM-E AMSTA-AR-FSS-D, BLDG. 94 AMSTA-AR-IMC, BLDG. 59 PICATINNY ARSENAL, NJ 07806-5000	1 1 1 1 1 1 2	COMMANDER U.S. ARMY TANK-AUTMV R&D COMMAND ATTN: AMSTA-DDL (TECH LIBRARY) WARREN, MI 48397-5000	1
DIRECTOR U.S. ARMY RESEARCH LABORATORY ATTN: AMSRL-DD-T, BLDG. 305 ABERDEEN PROVING GROUND, MD 21005-5066	1	COMMANDER U.S. MILITARY ACADEMY ATTN: DEPARTMENT OF MECHANICS WEST POINT, NY 10966-1792	1
DIRECTOR U.S. ARMY RESEARCH LABORATORY ATTN: AMSRL-WT-PD (DR. B. BURNS) ABERDEEN PROVING GROUND, MD 21005-5066	1	U.S. ARMY MISSILE COMMAND REDSTONE SCIENTIFIC INFO CENTER ATTN: AMSMI-RD-CS-R/DOCUMENTS BLDG. 4484 REDSTONE ARSENAL, AL 35898-5241	2
DIRECTOR U.S. MATERIEL SYSTEMS ANALYSIS ACTV ATTN: AMXSY-MP ABERDEEN PROVING GROUND, MD 21005-5071	1	COMMANDER U.S. ARMY FOREIGN SCI & TECH CENTER ATTN: DRXST-SD 220 7TH STREET, N.E. CHARLOTTESVILLE, VA 22901	1
		COMMANDER U.S. ARMY LABCOM, ISA ATTN: SLCIS-IM-TL 2800 POWER MILL ROAD ADELPHI, MD 20783-1145	1

NOTE: PLEASE NOTIFY COMMANDER, ARMAMENT RESEARCH, DEVELOPMENT, AND ENGINEERING CENTER,
BENÉT LABORATORIES, CCAC, U.S. ARMY TANK-AUTOMOTIVE AND ARMAMENTS COMMAND,
AMSTA-AR-CCB-O, WATERVLIET, NY 12189-4050 OF ADDRESS CHANGES.

	NO. OF COPIES		NO. OF COPIES
COMMANDER U.S. ARMY RESEARCH OFFICE ATTN: CHIEF, IPO P.O. BOX 12211 RESEARCH TRIANGLE PARK, NC 27709-2211	1	WRIGHT LABORATORY ARMAMENT DIRECTORATE ATTN: WL/MNM EGLIN AFB, FL 32542-6810	1
DIRECTOR U.S. NAVAL RESEARCH LABORATORY ATTN: MATERIALS SCI & TECH DIV WASHINGTON, D.C. 20375	1	WRIGHT LABORATORY ARMAMENT DIRECTORATE ATTN: WL/MNMF EGLIN AFB, FL 32542-6810	1

NOTE: PLEASE NOTIFY COMMANDER, ARMAMENT RESEARCH, DEVELOPMENT, AND ENGINEERING CENTER, BENÉT LABORATORIES, CCAC, U.S. ARMY TANK-AUTOMOTIVE AND ARMAMENTS COMMAND, AMSTA-AR-CCB-O, WATERVLIET, NY 12189-4050 OF ADDRESS CHANGES.